

Janus-faced influence of the Hund's rule coupling in strongly correlated materials.

Luca de' Medici,¹ Jernej Mravlje,^{2,3} and Antoine Georges^{2,4,5}

¹*Laboratoire de Physique des Solides, UMR8502 CNRS-Université Paris-Sud, Orsay, France*

²*Centre de Physique Théorique, École Polytechnique, CNRS, 91128 Palaiseau Cedex, France*

³*Jožef Stefan Institute, Jamova 39, SI-1000, Ljubljana, Slovenia*

⁴*Collège de France, 11 place Marcelin Berthelot, 75005 Paris, France*

⁵*Japan Science and Technology Agency, CREST, Kawaguchi 332-0012, Japan*

We show that in multi-band metals the correlations are strongly affected by the Hund's rule coupling, which depending on the filling promotes metallic, insulating or bad-metallic behavior. The quasiparticle coherence and the proximity to a Mott insulator are influenced distinctly and, away from single- and half-filling, in opposite ways. A strongly correlated bad-metal far from a Mott phase is found there. We propose a concise classification of 3d and 4d transition-metal oxides within which the ubiquitous occurrence of strong correlations in Ru- and Cr-based oxides, as well as the recently measured high Néel temperatures in Tc-based perovskites are naturally explained.

Hund's rules determine the ground-state of an isolated atom by accounting for the dependence of the Coulomb repulsion between electrons on their relative spin and orbital configurations. In insulating solids, their role is to select the relevant atomic multiplets, which are then coupled by inter-site magnetic interactions. In contrast, the effects of the Hund's rule coupling in metallic compounds are less understood. The difficulty lies in dealing with the localized (atomic) and itinerant characters of electrons on equal footing, a key issue for materials with strong electron correlations [1]. Despite increasing awareness of the physical relevance of the Hund's rule coupling for such materials[2–8], a global view is still lacking.

In this article, we fill this gap and provide a classification with respect to the number of electrons filling the active orbitals. We show that, aside from the case of a singly-occupied shell (where metallicity is favored[4, 8]), or a half-filled shell (where it promotes Mott insulating behaviour[9, 10]) the Hund's rule coupling induces conflicting tendencies and thus causes strong correlations far from the insulating state ('bad-metal' behavior). This picture explains the observed physical properties of a number of transition-metal oxides and allows for predictions on novel ones, such as Technetium compounds.

In order to describe all these possibilities and illustrate our key-point in a simple context, we consider a model of three identical bands with semicircular density-of-states of half-bandwidth D filled by N electrons per site. This is relevant, for example, to transition-metal oxides with cubic symmetry and a partially filled t_{2g} shell well separated from the empty e_g shell. The standard interaction Hamiltonian [1] can be written as:

$$H_{\text{int}} = (U - 3J) \frac{\hat{N}(\hat{N} - 1)}{2} - 2J\vec{S}^2 - \frac{1}{2}J\vec{T}^2 \quad (1)$$

where \hat{N} denotes total charge, \vec{S} spin and \vec{T} the angular momentum operators. U is the intra-orbital interaction and J is the Hund's rule coupling. The Hund's rule coupling favors, in decreasing order: configurations with parallel spins in different orbitals, with parallel spins in the

same orbital, and with opposite spins in the same orbital, maximizing S and then T . We solve the model using dynamical mean-field theory (DMFT)[11] which maps a correlated electron system onto a quantum-impurity problem: an effective atom coupled to a self-consistent environment. This approach handles the on-site atomic physics and the itinerant motion of electrons on equal footing. Both the limit of an isolated atom with its multiplet structure and that of a non-interacting band are correctly reproduced.

In Fig. 1, we display the quasiparticle spectral weight Z as a function of coupling U , for several values of J , in the paramagnetic state. Z characterizes the degree of correlations of the metallic state. For example, the Drude weight measured from optical conductivity is proportional to Z [11]. It also sets the energy/temperature scale T^* above which the lifetime of quasiparticles becomes short and coherence is lost. Z and T^* diminish progressively as U/D is increased and a vanishing Z signals the Mott insulating state, reached for $U > U_c$. We observe that the case of one-electron ($N = 1$) is in striking contrast to the case of a half-filled shell ($N = M = 3$): upon increasing J/U the critical coupling U_c in the former is increased[8] while in the latter it is reduced[9, 10]. Correspondingly, for a fixed U in the metallic phase, Z increases with J for $N = 1$ while it decreases for $N = M$. Hence, as summarized in Table I, correlations are increased by the Hund's rule coupling for a half-filled shell, and diminished for a singly-occupied one.

In contrast, we find that the Hund's rule coupling has a more complex influence in the case of two electrons (or two holes) in 3 orbitals. On the one hand, the critical coupling U_c is strongly increased (and the Mott gap reduced) at the largest values of J/U . As a result, the range of coupling U/D with metallic behaviour is enlarged as compared to the case with $J = 0$. On the other hand, for a wide range of coupling strengths, Z is suppressed upon increasing J [7, 12, 13]. To accommodate these antagonistic effects, Z displays a long tail as a function of U . The small values of Z found there

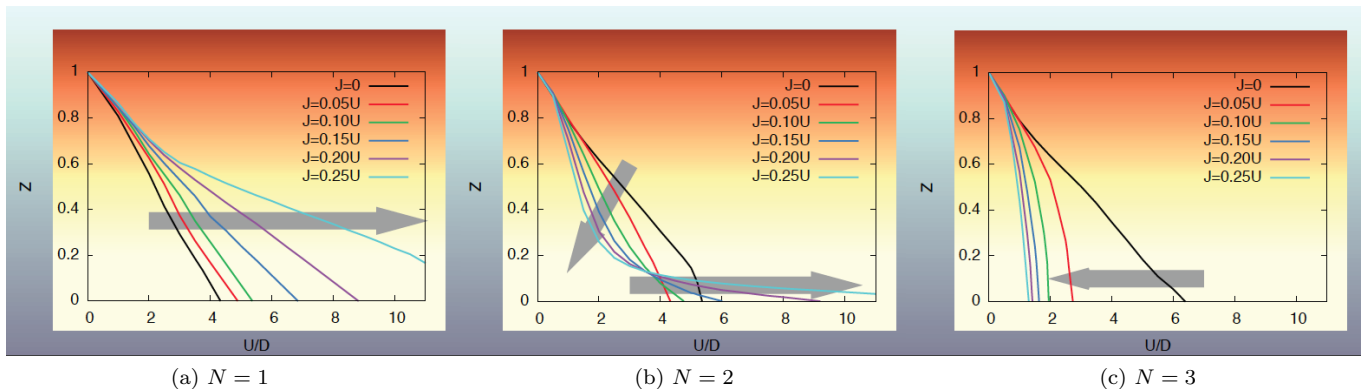


Figure 1: Quasiparticle weight Z vs. U for $N = 1, 2, 3$ electrons in $M = 3$ orbitals. The grey arrows indicate the influence of an increasing Hund's rule coupling J/U .

Number N of electrons in M orbitals	Degeneracy of atomic ground-state	Mott gap	Correlations	Materials behaviour promoted by J
one electron or one hole ($N = 1, 2M - 1$)	unaffected	reduced	diminished	metallic
half-filled ($N = M$)	reduced	increased	increased	insulating
All other cases ($N \neq 1, M, 2M - 1$)	reduced	reduced	Conflicting effect (see text)	bad metallic

Table I: The effects of an increasing Hund's rule coupling on the degree of correlations.

indicate a very low quasiparticle coherence scale T^* , below which the system is expected to show a conventional Fermi liquid physics. An incoherent regime with a Curie-like magnetic response[3] and bad-metal behavior [3, 7] is found for temperatures above T^* (see the Supporting online information[14]). This was reported in Ref. [3] and coined 'spin-freezing' regime. These considerations are not specific to 2 electrons in 3 orbitals: the Hund's coupling is 'Janus-faced' for N electrons in M degenerate orbitals, except for a singly-occupied or half-filled band, as summarized in Table. I.

We calculated also away from integer fillings and display the data as a contour plot of the quasiparticle weight as a function of coupling strength U/D and band filling, for a fixed typical value of the ratio J/U (Fig. 2). The extended region of strongly-correlated/bad metallic behaviour (small Z) around $N = 2$ appears clearly. In contrast, the half-filled case favors insulators (except at weak U/D) and the single-electron case favors good metals (except at strong U/D).

These numerical results can be corroborated and explained by analytical considerations in the simplified limits. In order to understand the influence of J on the Mott gap, we start from the limit of an isolated atom. The charge gap $\Delta_{\text{at}} = E_{\text{at}}(N + 1) + E_{\text{at}}(N - 1) - 2E_{\text{at}}(N)$ takes two different values depending on whether the relevant orbitals are half filled or not; $\Delta_{\text{at}} = U - 3J$ for $N < M$ or $N > M$ and $\Delta_{\text{at}} = U + (M - 1)J$ for $N = M$.

Including hopping perturbatively leads to a correction $\Delta_{\text{Mott}} = \Delta_{\text{at}} - cD + \dots$, where c is of order unity. Hence, we see that the Mott gap is increased by J (and U_c decreased) at half-filling[9, 10], while it is decreased in all other cases[4, 8]. This localized limit explains the distinction between $N = 3$ and $N = 1$ (and the insulating side of $N = 2$) but does not account for the bad-metal/small- Z part of the phase diagram around $N = 2$.

To understand this regime we consider the itinerant limit. Studying a correlated metallic phase within DMFT translates mainly in characterizing the coherence scale of the effective impurity problem (self-consistent atom). Here we focus on how it is affected by the Hund's coupling. The key distinction between different cases is the degeneracy of the atomic ground-state which is, except for a single electron or hole, reduced by J , as the state with aligned angular momenta is selected (Table S1 in the Supporting online information[14]). Lower degeneracy enhancing the quantum fluctuations and weaker tunneling from/onto the composite object suppress the coherence scale[15–19], which corresponds to the Kondo scale of the effective impurity model below which the atomic multiplet is screened out. Further numerical and analytical results are given in the Supporting online information[14].

Now we examine how the different influences of the Hund's rule coupling are manifested in the physical properties of transition-metal oxides. First, a word of warn-

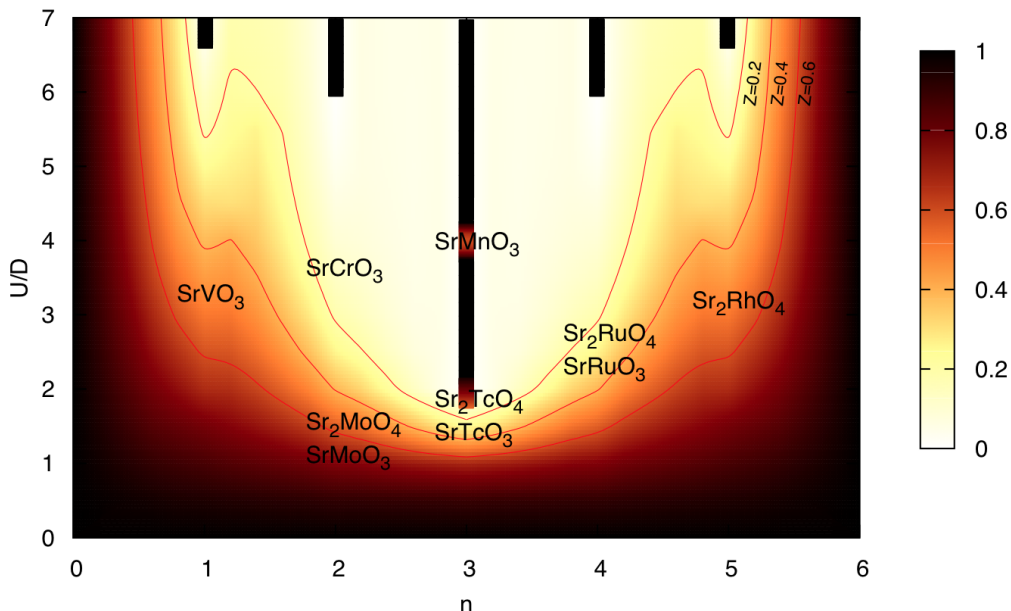


Figure 2: Quasiparticle weight Z in a model with 3 orbitals, for $J/U = 0.15$, as a function of the interaction strength U and the number of electrons - from empty (0) to full (6). Darker regions correspond to good metals and lighter regions to bad metals. The black bars signal the Mott-insulating phases. One notes that, among integer fillings, the case of 2 electrons (2 holes) displays bad-metal behaviour in an extended range of coupling. Specific materials are schematically placed on the diagram (see text).

ing. Often these materials do not have perfect cubic symmetry. The distortions mix the orbitals, reduce the bandwidths and induce crystal fields which lower the atomic degeneracy further. These effects usually enhance the correlations and promote insulating behavior, which can often be described by an effective model with a smaller number of orbitals (as some are emptied or filled by the crystal fields) [20–22]. For illustrative purposes, we choose a set of materials indicated on Fig. 2. In [14], the discussion is extended to other materials for which the lifting of orbital degeneracies is stronger.

We begin with oxides of 3d transition metals with a half-filled t_{2g} shell, such as SrMnO_3 and LaCrO_3 . A typical ratio of the Coulomb repulsion to half bandwidth for these materials is $U/D \simeq 4\text{eV}/1\text{eV}$. This exceeds substantially the insulating limit for this case, explaining why no metallic $3t_{2g}^3$ oxides are known[1, 23]. Conversely, at a comparable value of U/D , the $3t_{2g}^1$ cubic SrVO_3 is a moderately correlated metal with $Z^{-1} = m^*/m \simeq 2$ [1]. LDA+DMFT explicitly demonstrates (see [14]), that SrVO_3 would be significantly more correlated[4] were it not for the decorrelating action of Hund’s rule at this

filling. For $3t_{2g}^2$ materials, still within the same range of U/D (Fig. 2), strongly correlated bad-metal behavior caused by the Janus-faced action of J is found. Observable signatures of bad-metals are large values (beyond the Mott limit [24]) of the non- T^2 but metallic-like resistivity in the extended temperature range above a very low T^* and a large, poorly screened moment, prone to itinerant magnetism. A possible realization among 3d oxides is SrCrO_3 [25, 26].

Oxides of 4d transition metals are characterized by smaller values of $U/D \simeq 2$, due to the larger bandwidths and smaller screened interaction associated with the more extended 4d orbitals. We consider the series SrMO_3 and Sr_2MO_4 with $M = \text{Mo}, \text{Tc}, \text{Ru}, \text{Rh}$ (Fig.2). The Technetium compounds are special among those: they are located very close to the metal/insulator transition. We are not aware of transport measurements on these compounds, but a recent study[27] indeed reports antiferromagnetism with a very large Néel temperature $T_N \simeq 1000$ K for SrTcO_3 . Simple model considerations do suggest that the vicinity of the Mott critical coupling leads to largest values of T_N . As a test of our classifica-

tion, we predict that Sr_2TcO_4 is an insulator or a very strongly correlated metal.

The Mo-, Ru- and Rh- based compounds are metallic. For tetragonal 214's an orbital average of the measured values yields $Z^{-1} = m^*/m \sim 2$ for Sr_2MoO_4 ($4t_{2g}^2$) [28], ~ 4 for Sr_2RuO_4 ($4t_{2g}^4$) [1] and ~ 2 for Sr_2RhO_4 ($4t_{2g}^5$) [29]. These variations are explained by a closer examination of the electronic structure of these materials. For example, values for Sr_2MoO_4 and Sr_2RuO_4 differ because the t_{2g} density of states is not particle-hole symmetric: the ruthenate has the Fermi level close to a van Hove singularity and therefore a smaller effective bandwidth[7]. On the other hand, relatively large correlations found in rhodates occur due to the bandwidth narrowing and the orbital polarization induced by rotations of the octahedra. In the regime of weak to moderate correlations with 2 electrons (Fig. 1), Z has a steep dependence on U/D : this explains that SrMoO_3 has an unusually large metallic conductivity among oxides[30]. 4d materials can be driven also to the extreme bad metal regime by rotation-induced narrowing of the bandwidths achieved by Ca substitution. An example is $\text{Sr}_{1-x}\text{Ca}_x\text{RuO}_3$, which at $x = 1$ has $m^*/m > 5$ and remains incoherent down to lowest temperatures measured [31].

There is thus a class of Hund's correlated materials which are strongly correlated but driven by J rather than the proximity to a Mott insulator. In this respect, we note that the importance of the Hund's rule coupling has also been emphasized for the iron-based superconductors[2, 5, 6]. With 6 electrons in 5 active orbitals, the bad-metal behaviour observed for these materials can be attributed to the conflicting action of the Hund's rule coupling. This puts pnictides on the map of Hund's correlated material along with SrCrO_3 and SrRuO_3 but also raises important questions. What is the nature of such materials above the coherence scale and how do they differ from materials close to the Mott transition? How are the instabilities to magnetism and superconductivity affected?

We are grateful to S. Biermann, M. Capone, A. Fujimori, E. Gull, K. Haule, M. Imada, A. Kapitulnik, G. Kotliar, C. Martins, I. Mazin, A. J. Millis, Y. Tokura, D. van der Marel, L. Vaugier and P. Werner for useful discussions. A.G. acknowledges the hospitality of the Université de Genève (DPMC) and the support of MANEP, and J.M. that of Rutgers University. This work was supported by the Partner University Fund, the Agence Nationale de la Recherche (ANR-09-RPDOC-019-01 and ANR-2010-BLAN-040804), the RTRA Triangle de la Physique and the Slovenian Research Agency (under contract J1-0747). Computer time was provided by IDRIS/GENCI under Grant 2011091393.

-
- [1] M. Imada, A. Fujimori, and Y. Tokura, *Rev. Mod. Phys.*, **70**, 1039 (1998).
 - [2] K. Haule and G. Kotliar, *New J. Phys.*, **11**, 025021 (2009).
 - [3] P. Werner, E. Gull, M. Troyer, and A. J. Millis, *Phys. Rev. Lett.*, **101**, 166405 (2008).
 - [4] P. Werner, E. Gull, and A. J. Millis, *Phys. Rev. B*, **79**, 115119 (2009).
 - [5] M. D. Johannes and I. I. Mazin, *Phys. Rev. B*, **79**, 220510 (2009).
 - [6] M. Aichhorn, S. Biermann, T. Miyake, A. Georges, and M. Imada, *Phys. Rev. B*, **82**, 064504 (2010).
 - [7] J. Mravlje, M. Aichhorn, T. Miyake, K. Haule, G. Kotliar, and A. Georges, *Phys. Rev. Lett.*, **106**, 096401 (2011).
 - [8] L. de' Medici, *Phys. Rev. B*, **83**, 205112 (2011).
 - [9] J. Bünenmann, W. Weber, and F. Gebhard, *Phys. Rev. B*, **67**, 6896 (1998).
 - [10] J. E. Han, M. Jarrell, and D. L. Cox, *Phys. Rev. B*, **58**, R4199 (1998).
 - [11] A. Georges, G. Kotliar, W. Krauth, and M. J. Rozenberg, *Rev. Mod. Phys.*, **68**, 13 (1996).
 - [12] T. Pruschke and R. Bulla, *Eur. Phys. J. B*, **44**, 217 (2005).
 - [13] P. Lombardo, A.-M. Daré, and R. Hayn, *Phys. Rev. B*, **72**, 245115 (2005).
 - [14] L. de' Medici, J. Mravlje, and A. Georges, , Supplementary online material.
 - [15] I. Okada and K. Yosida, *Prog. Theor. Phys.*, **49**, 1483 (1973).
 - [16] H. Kusunose and K. Miyake, *Journal of the Physical Society of Japan*, **66**, 1180 (1997).
 - [17] Y. Yanase and K. Yamada, *Journal of the Physical Society of Japan*, **66**, 3551 (1997).
 - [18] S. Yotsuhashi, H. Kusunose, and K. Miyake, *Journal of the Physical Society of Japan*, **70**, 186 (2001).
 - [19] A. H. Nevidomskyy and P. Coleman, *Phys. Rev. Lett.*, **103**, 147205 (2009).
 - [20] N. Manini, G. E. Santoro, A. dal Corso, and E. Tosatti, *Phys. Rev. B*, **66**, 115107 (2002).
 - [21] E. Pavarini, S. Biermann, A. Poteryaev, A. I. Lichtenstein, A. Georges, and O. K. Andersen, *Phys. Rev. Lett.*, **92**, 176403 (2004).
 - [22] A. I. Poteryaev, M. Ferrero, A. Georges, and O. Parcollet, *Phys. Rev. B*, **78**, 045115 (2008).
 - [23] J. Torrance, P. Lacorre, C. Asavaroengchai, and R. Metzger, *Physica C*, **182**, 351 (1991).
 - [24] V. J. Emery and S. A. Kivelson, *Phys. Rev. Lett.*, **74**, 3253 (1995).
 - [25] B. L. Chamberland, *Solid State Comm.*, **5**, 663 (1967).
 - [26] J.-S. Zhou, C.-Q. Jin, Y.-W. Long, L.-X. Yang, and J. B. Goodenough, *Phys. Rev. Lett.*, **96**, 046408 (2006).
 - [27] E. E. Rodriguez, F. Poineau, A. Llobet, B. J. Kennedy, M. Avdeev, G. J. Thorogood, M. L. Carter, R. Seshadri, D. J. Singh, and A. K. Cheetham, *Phys. Rev. Lett.*, **106**, 067201 (2011).
 - [28] S.-I. Ikeda, N. Shirakawa, H. Bando, and Y. Ootuka, *Journal of the Physical Society of Japan*, **69**, 3162 (2000).
 - [29] R. S. Perry, F. Baumberger, L. Balicas, N. Kikugawa, N. J. C. Ingle, A. Rost, J. F. Mercure, Y. Maeno, Z. X. Shen, and A. P. Mackenzie, *New Journal of Physics*, **8**,

- 175 (2006).
- [30] I. Nagai, N. Shirakawa, I. Shin-ichi, R. Iwasaki, H. Nishimura, and M. Kosaka, *Appl. Phys. Lett.*, **87**, 024105 (2005).
 - [31] G. Cao, S. McCall, M. Shepard, J. E. Crow, and R. P. Guertin, *Phys. Rev. B*, **56**, R2916 (1997).
 - [32] P. Werner, A. Comanac, L. de' Medici, M. Troyer, and A. J. Millis, *Phys. Rev. Lett.*, **97**, 076405 (2006).
 - [33] M. Aichhorn *et al.*, *Phys. Rev. B*, **80**, 085101 (2009).
 - [34] Y. Nishikawa, D. J. G. Crow, and A. C. Hewson, *Phys. Rev. B*, **82**, 245109 (2010).
 - [35] R. Žitko, , <http://auger.ijs.si/ljubljana/>.
 - [36] M. Caffarel and W. Krauth, *Phys. Rev. Lett.*, **72**, 1545 (1994).
 - [37] M. Jarrell and T. Pruschke, *Phys. Rev. B*, **49**, 1458 (1994).
 - [38] F. Baumberger, N. J. C. Ingle, W. Meevasana, K. M. Shen, D. H. Lu, R. S. Perry, A. P. Mackenzie, Z. Hussain, D. J. Singh, and Z.-X. Shen, *Phys. Rev. Lett.*, **96**, 246402 (2006).
 - [39] B. J. Kim, J. Yu, H. Koh, I. Nagai, S. I. Ikeda, S.-J. Oh, and C. Kim, *Phys. Rev. Lett.*, **97**, 106401 (2006).
 - [40] P. Werner and A. J. Millis, *Phys. Rev. Lett.*, **99**, 126405 (2007).
 - [41] M. De Raychaudhury, E. Pavarini, and O. K. Andersen, *Phys. Rev. Lett.*, **99**, 126402 (2007).
 - [42] S. Nakatsuji, D. Hall, L. Balicas, Z. Fisk, K. Sugahara, M. Yoshioka, and Y. Maeno, *Phys. Rev. Lett.*, **90**, 137202 (2003).

Supplementary Information

MODEL CALCULATIONS

The 3-band model that we solve in this work can be formulated in term of a tight-binding hamiltonian $H = H_{\text{kin}} + H_{\text{int}}$ where for the kinetic energy term we take nearest-neighbor hopping amplitudes t :

$$H_{\text{kin}} = -t \sum_m \sum_{\langle ij \rangle, \sigma} (d_{im\sigma}^\dagger d_{jm\sigma} + \text{h.c.}). \quad (2)$$

Here $d_{im\sigma}^\dagger$ creates an electron at site i with spin σ in orbital m . Each one of the degenerate bands in this model has a semicircular density of states of half-bandwidth D .

The interaction, in the standard Kanamori form [1] reads

$$\begin{aligned} H_{\text{int}} = & U \sum_m n_{m\uparrow} n_{m\downarrow} + \\ & + \sum_{m < n, \sigma} [(U - 2J)n_{m\sigma} n_{n\bar{\sigma}} + (U - 3J)n_{m\sigma} n_{n\sigma}] \\ & - J \sum_{m < n} [d_{m\uparrow}^\dagger d_{m\downarrow} d_{n\downarrow}^\dagger d_{n\uparrow} + d_{m\uparrow}^\dagger d_{m\downarrow}^\dagger d_{n\uparrow} d_{n\downarrow} + \text{h.c.}] \\ \stackrel{t_{2g}}{=} & (U - 3J) \frac{\hat{N}(\hat{N} - 1)}{2} + \frac{5}{2} J \hat{N} - 2J \vec{S}^2 - \frac{1}{2} J \vec{T}^2. \end{aligned} \quad (3)$$

The last equality holds only for the t_{2g} orbitals, but the rest of the Hamiltonian remains valid also if m runs only over e_g orbitals. For t_{2g} orbitals it differs from Eq.(1) in the main text for a term $5/2J\hat{N}$, a simple shift in the chemical potential.

The model calculations were performed within the dynamical mean-field theory (DMFT)[11]. In this approach, correlated electron systems are mapped onto a quantum-impurity problem: an effective atom coupled to a self-consistent environment. Both the limit of an isolated atom with its multiplet structure and that of a non-interacting band are correctly reproduced.

The associated impurity model was solved using the zero-temperature exact diagonalization (ED) (see e.g. [11]) and the continuous-time quantum Monte carlo (CTQMC) [32] methods. 9 bath sites were used in ED calculations, 10^9 Monte Carlo cycles per iteration were used in CTQMC calculations at lowest $kT = D/400$. By comparing results of both methods (see Supplementary Information) we estimate the typical error in Z as $< 10\%$ for $Z \gtrsim 0.1$. For lower Z the coherence scale is smaller than the energy resolution of the employed methods and the results should be taken as indicative. We expect the error in U_c to be $< 10\%$. The material trends were verified by LDA+DMFT calculations based on the implementation described in [33].

SPECTRUM AND DEGENERACIES OF THE ISOLATED ATOM

In Table S1 we report the spectrum and the degeneracies of the t_{2g} Hamiltonian described by Eq.(1) in the main text. Except for the case $N = 1$, the degeneracy in every sector is reduced by J .

N	S	T	Degeneracy = $(2S + 1)(2T + 1)$	Energy
0	0	0	1	0
1	1/2	1	6	$-\frac{5}{2}J$
2	1	1	9	$(U - 3J) - 5J$
2	0	2	5	$(U - 3J) - 3J$
2	0	0	1	$(U - 3J)$
3	3/2	0	4	$3(U - 3J) - \frac{15}{2}J$
3	1/2	2	10	$3(U - 3J) - \frac{9}{2}J$
3	1/2	1	6	$3(U - 3J) - \frac{5}{2}J$

Table S1: Eigenstates and eigenvalues of the t_{2g} Hamiltonian in the atomic limit. The boxed numbers denote the ground-state degeneracies for $J > 0$.

INSIGHTS FROM THE IMPURITY MODEL

The influence of the Hund's coupling on correlations in the impurity model has been noticed and analysed in several studies, e.g. [15–18, 34]. We follow Ref. [19] and consider a set of Hund's coupled Kondo problems defined by the Hamiltonian $H = -J(\sum_{\alpha=1}^N \vec{S}_\alpha)^2 + J_K \sum_\alpha \vec{S}_\alpha \cdot \vec{s}_\alpha^c + \sum_{k\alpha\sigma} \varepsilon_k c_{k\alpha\sigma}^\dagger c_{k\alpha\sigma}$, with J_K the Kondo coupling between the spin density of conduction electrons \vec{s}_α^c to the local spins \vec{S}_α . In the limit of vanishing Hund's coupling, one has N uncoupled impurity problems with the Kondo temperature $T_{K0} = D \exp(-1/\rho J_K)$ where ρ is the density of states of the conduction electrons. In the opposite limit of large Hund's coupling a composite object with large spin $S = N/2$ is formed and in this limit one can write $\vec{S}_\alpha \sim \vec{S}/N$ (a relation verified by summing over α). One thus faces a N -channel Kondo problem coupled to a spin S with a reduced Kondo coupling J_K/N . As a result, the Kondo scale $T_K = D \exp(-N/(\rho J_K)) = T_{K0}(T_{K0}/D)^{N-1}$ is reduced and the correlations are enhanced.

This simple analysis is confirmed by numerical renormalization-group calculations. In Fig. S1 we plot the impurity contribution to the susceptibility for two Hund's rule coupled Kondo impurities with $S = 1/2$ described by the Hamiltonian

$$H = -J \left(\sum_{\alpha=1,2} \vec{S}_\alpha \right)^2 + J_K \sum_\alpha \vec{S}_\alpha \cdot \vec{s}_\alpha^c + \sum_{k\alpha\sigma} \varepsilon_k c_{k\alpha\sigma}^\dagger c_{k\alpha\sigma}, \quad (4)$$

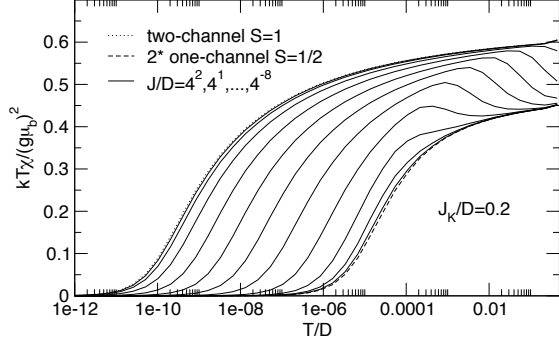


Figure S1: Local moment $kT\chi/(g\mu_B)^2$ as a function of temperature T/D . As the Hund's coupling J increases the characteristic temperature drops.

with J_K the Kondo coupling between the spin density of conduction electrons \bar{s}_α^c to the local spins \bar{S}_α . A flat density of states is taken for the conduction electrons. The Hamiltonian is solved using the numerical-renormalization group method [35].

Note that with increasing J the low-energy characteristic scale below which the impurity is screened (i.e. the Kondo temperature) diminishes linearly for J larger than the Kondo temperature of the $J = 0$ problem but smaller than J of the order of bandwidth, in agreement with the perturbative-RG analysis presented in [17, 19]. Large- J results are interpreted as discussed in the main text.

COMPARISON BETWEEN ED AND CTQMC

The quasi-particle spectral weights Z are extracted from ED [36] and CTQMC [32] simulations using polynomial fits of the electron self-energies for the lowest Matsubara frequencies. ED is a zero-temperature method (although finite-temperature-like effects appear due to the discretization of the bath), therefore a linear approximation gives good results. In contrast, in CTQMC, the (zero-temperature) Z is estimated from data at higher temperatures and the polynomial fits use few Matsubara frequencies (we typically use 4th order polynomial fit to 6 Matsubara frequencies). Z converges only when the temperature is lowered below the coherence scale [37]. The convergence of Z as well as the difference between the ED and CTQMC results are presented in Fig. S2. Note that in this data, representative of the Janus-faced regime, the coherence temperature diminishes rapidly with U and reaches values we cannot reach numerically already for $U \sim 4D$, still far from the $U_c \sim 6D$.

Small values of Z indicate also a very low coherence scale T^* .

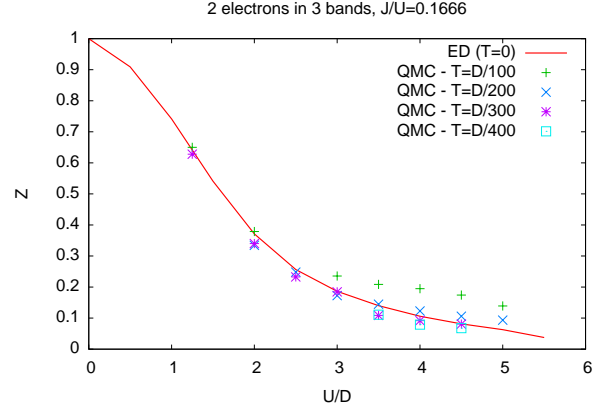


Figure S2: Comparison between ED and CTQMC data.

For concreteness, we define T^* by $\Gamma = kT^*$ and thus identify it with the temperature above which the scattering rate Γ (that grows with temperature) exceeds the typical energy (= temperature) of a quasiparticle. [7].

For the case of 2 electrons in 3 bands and $J/U=0.15$ we find $T^* \sim 50\text{K}$ for $Z \sim 0.1$; $T^* \lesssim 20\text{K}$ for $Z \lesssim 0.05$. The scattering rates in the $T > T^*$ regime reach large values and increase monotonously with temperature, a characteristics of the bad-metals [24]. While the low temperature Fermi liquid behavior is similar for all the fillings, we find, as in Ref. [3], a different response at higher temperatures (or higher frequencies) away from single- and half-filling.

TWO-BAND MODEL

We solved also the two-band Hamiltonian, relevant to materials with complete t_{2g} and partially filled e_g shells as well as to other materials, for instance $4t_{2g}^5 \text{Sr}_2\text{RhO}_4$ in which due to the rotations the xy -orbital is pushed below the Fermi level [38, 39]. In Fig. S3 we display the two-band analogue of the data presented in Fig. 2 of the main text.

The Mott transition occurs for the singly-occupied and the half-filled case as discussed for the corresponding cases in the three-orbital model and presented on panels a and c of Fig. 1 in the main text. In the singly-occupied case the Hund's coupling has no effect on the ground state degeneracy but reduces the Mott gap and promotes metallicity. On the contrary, in the half-filled case the gap is increased. Even in the absence of the increase of the gap the coherence scale would drop as $S = 1$ is formed (due to reduced degeneracy and suppressed tunneling). Both effects reduce the coherence temperature, enhance correlations and promote the Mott insulating state. There is no integer filling at which J

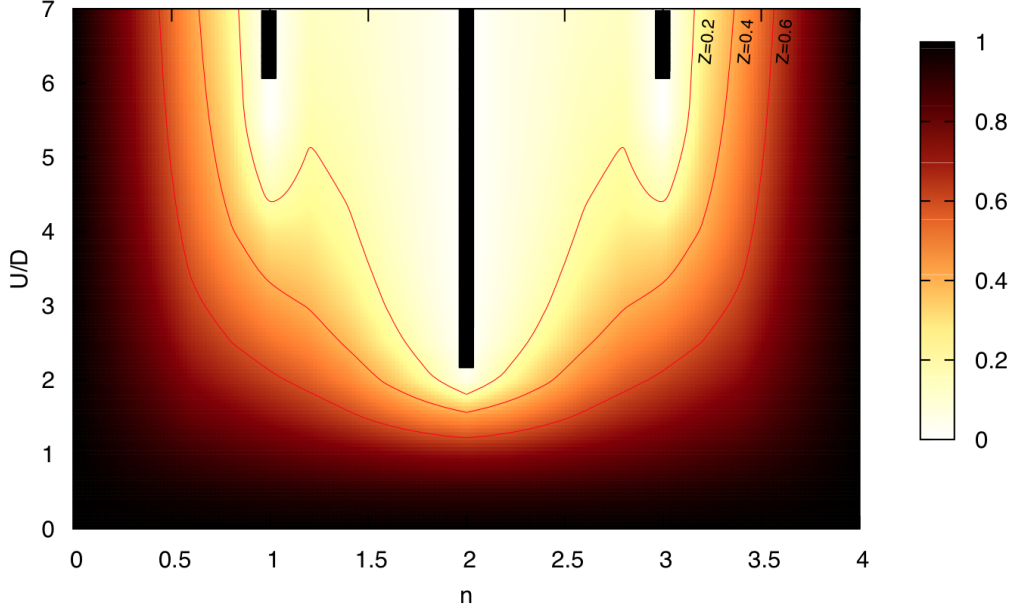


Figure S3: Quasiparticle weight Z for a model with 2 orbitals, for $J/U = 0.15$, as a function of the interaction strength U and filling - from empty (0) to full (4). Darker regions correspond to good metals and lighter regions to bad metals. The black bars signal the Mott insulating phase.

has antagonistic effects and bad metals are found only in close proximity to the Mott insulator.

Note also that, except near half filling, higher correlations signalled by lower values of Z are found, compared to the three-band case. This can be related to the lower orbital degeneracy. Correspondingly, the U_c for the transition to the Mott insulator is also smaller for the single electron/single hole case, while for half-filling it is instead slightly larger (for this value of $J/U = 0.15$). This happens because the Mott gap at half-filling in the three-orbital model increases as $2J$ whereas in the present case only as J (see main text).

LDA+DMFT SIMULATIONS

To verify that the effects of the Hund's coupling can account for different behavior of materials, which are chemically and structurally close, we performed LDA+DMFT simulations within the framework described in [33] on a set of materials noted on Fig. 2 of the main text. We constructed the t_{2g} Wannier-like orbitals from the energy window containing the t_{2g} bands.

SrVO_3 is found to be a moderately correlated material

– as seen also in experiments [1] – precisely due to the decorrelating influence of the Hund's rule coupling in the singly occupied regime. For $U = 4$ we found that by diminishing J from the realistic value 0.7eV to 0, $Z^{-1} = m^*/m$ increases from 2 to 3. At $U = 5\text{eV}$ and $J = 0$ a Mott insulator is found, while for realistic $J = 0.7\text{eV}$ the material remains a moderately correlated metal with $m^*/m = 3$.

The $4t_{2g}^2$ oxide Sr_2MoO_4 is an electronic analogue of $4t_{2g}^4$ Sr_2RuO_4 but found in experiments far more coherent [28]. For Sr_2MoO_4 we used same interaction parameters $U = 2.3\text{eV}$ and $J = 0.4\text{eV}$ as for Sr_2RuO_4 [7]. Despite the particle-hole symmetry relating the electron contents of the two compounds, Sr_2MoO_4 has $m^*/m \sim 2$, twice smaller than $m^*/m \sim 4$ for the Ru-compound. The distinction occurs because the band structure are not particle-hole symmetric and the band-value of the density of states close to the Fermi level is for Sr_2MoO_4 much smaller, making it less sensible to the influence of interaction. The SrMoO_3 is due to cubic symmetry and related wider bands found even more coherent. The data on other materials will be reported separately.

REMARKS ON CRYSTAL-FIELD, SPIN-ORBIT AND CHARGE-TRANSFER EFFECTS

Here we discuss other important aspects determining how correlated a certain material is, which are only implicitly (through selecting the effective degeneracy and the effective bandwidth) contained in simplified model Hamiltonians, e.g. Eq. (1) of the main text.

Lowering of the crystal symmetry from cubic induces the splitting of the t_{2g} orbitals, leading to orbital polarization, diminishes the bandwidths and introduces significant orbital mixing. The correlations are often enhanced and especially for $3d$ oxides the distorted materials are insulating [20–22, 40].

The effect of structural distortions and resulting lowering of degeneracy are crucial in order to account for the insulating nature of $3t_{2g}^1$ oxides such as LaTiO_3 or YTiO_3 [21] and $3t_{2g}^2$ oxides such as LaVO_3 or YVO_3 [41].

For $4t_{2g}^2$ materials the insulating state is induced only exceptionally, e.g. in Ca_2RuO_4 [31] and we believe that the other cases in which the structure is distorted are reasonably well described within Eq (1) but with reduced bandwidths, leading to the pronounced bad-metal behavior found in these materials[42].

An analogous effect can appear due to the spin-orbit coupling, relevant for the late 4d and 5d transition metal elements. The orbital polarization and the related lower number of active orbitals might occur also here, thus en-

hancing correlations (C. Martins and S. Biermann, private communication).

For a large part of the article we have assumed that crystal-field effects are large enough to separate the e_g and t_{2g} manifolds. On the contrary when the crystal-field effects are small compared to the Hund’s coupling, orbital polarization is suppressed and all five d-orbitals are partially filled as it happens in the case of Iron superconductors cited in the main text. In such situations, albeit generalized to a higher number of active orbitals, the effects of Hund’s coupling outlined in this article should hold, leading to the filling-dependent promotion of metallic (for single electron/single hole), Mott insulating (for the half-filled case) or bad metallic behaviours (for all other fillings).

In other cases, such as for Manganites, a small crystal field and a large Hund coupling can promote localized t_{2g} electrons in high-spin states and double exchange physics.

Finally, some care in finding a correct low energy Hamiltonian and applying our arguments must be taken in describing materials which are of the charge-transfer type, e.g. oxides of the late 3d transition metals such as SrCoO_3 , in which the Mott gap is defined by excitation of holes in the oxygen bands. The influence of J in tuning the Mott gap in these cases is limited by the presence of these bands, while the suppression of the coherence temperature still applies for non-singly-occupied cases.